論文

수지이동 성형공정중 금형충전에 대한 연구 I. 수치모사 연구

최미애** · 이미혜*** · 이기준* · 이승종*

Studies on the Mold Filling in the Resin Transfer Molding Process I. Numerical Simulations

Mi Ae Choi**, Mi Hye Lee***, Ki-Jun Lee*, and Seung Jong Lee*

초 록

수지이동성형(RTM)에서 금형충전단계를 수치모사할 수 있는 컴퓨터 프로그램을 개발하였다. RTM 공정의 수지흐름의 특징인 수지선단의 진전과 불규칙한 금형 경계면을 해석하기 위해서 유한요소법과 수치메쉬생성 기법이 사용되었다. RTM 공정의 설계와 운전을 위해선 물질상수, 금형구조, 충전조건과 같은 여러 조업 변수에 대한 영향이 선행적으로 고찰되어야 한다. 수치모사로부터 얻은 결과들은 이러한 중요한 변수들과 금형설계를 최적화하기 위한 정보와의 연관성을 해석하는데 중요한 역할을 해주고 있다. 금형충전에 미치는 영향을 조사하기 위하여 공정변수를 변화시키면서 수치모사를 수행하였다. 본 연구에서 개발된 프로그램의 유용성을 입증하기 위하여 복잡하고 다양한 형태의 금형구조에도 적용해 보았다.

ABSTRACT

Computational program for numerical simulations of the mold filling in the resin transfer molding(RTM) process was developed. The finite element method and the numerical mesh generation technique were used to deal with the problem of the advancement of resin front and the irregularly-shaped boundaries in the RTM process. The design and operation of RTM require an understanding of various parameters, such as materials properties, mold geometry, and mold filling conditions. The results from numerical simulation provided a potential tool for analyzing the relationships among the important parameters and the information for optimizing mold design. Numerical simulations were undertaken varying these processing parameters in order to investigate the effects on the mold filling. The program was also applied to the molds with complicated geometry and with varying thickness to illustrate its capability.

* 서울대학교 화학공학과
** 국립기술품질원
*** 부산지방중소기업청

1. INTRODUCTION

Resin transfer molding(RTM) refers to a number of different fabrication processes which involve the transfer of catalyzed resin into an enclosed mold cavity containing a previously positioned reinforcement preform and the subsequent curing.

RTM process has the following advantages ;

(a) Very large and complex shapes can be made efficiently and inexpensively.

(b) Production times are much shorter than lay-up.

(c) Clamping pressure is low compared to matched-die molding.

(d) Surface definitions are superior to that with lay-up.

(e) Inserts and special reinforcements can be added easily.

RTM is a versatile and efficient process that is gaining popularity in almost all areas of the composite industry. Applications for RTM using advanced composites cover the full ranges of commercial and military aerospace parts, automotive, and consumer products. A good understanding of the manufacturing process and material properties is necessary to accomplish good structural composite design[1-5].

Mold filling stage in RTM process is a very important process and the contemporary research being done in this field is mainly the numerical simulation and experimental verification of the resin flow. Coulter et al.[6-8] simulated two-dimensional resin impregnation processes using the numerical method of boundary-fitted coordinates numerical grid generation along with a stream-function formulation based on assumption of Darcy' s flow through porous media. Gauvin et al.[9-11] developed a numerical model based on Darcy' s law and on the numerical generation of boundary-fitted coordinate system. The computer program permits to simulate the filling of two-dimensional molds of arbitrary shapes and the resin pressure distribution and the resin front positions can be obtained at each time step. A somewhat different approach was taken by Bruschke and Advani[12,13] in their effort to model the RTM process. They presented a numerical solution based on a finite element/control volume method to calculate the flow pattern for mold filling in anisotropic media.

In the present study, the mathematical equation is developed to model a resin flow in thin cavities preplaced with fiber mats. The finite element technique is used to solve the governing equations and this technique offers the capability of modelling the moving flow front in a computationally efficient manner. The finite element method with numerical mesh generation used in this study is efficient in the accuracy in comparison with other numerical techniques.

Using the computational program developed in present study, the numerical simulation is carried out under variation of processing and material parameters. Through the numerical results of mold filling the affects of process parameters are investigated and the optimization of mold design is provided.

2. MATHEMATICAL MODELLING

For an incompressible fluid, the continuity equation can be reduced to the form.

$$\frac{\partial u}{\partial x}+\frac{\partial v}{\partial y}+\frac{\partial w}{\partial z}=0 \cdots\cdots\cdots\cdots\cdots\cdots\cdots\cdots\cdots\cdots\cdots\cdots(1)$$

Based on the lubrication approximation, the generalized Hele-Shaw flow model which provides simplified governing equations for the thin cavity was applied in this study. The governing equation can be simplified as follows ;

$$\frac{\partial}{\partial x}(h(x,y)\cdot\bar{u})+\frac{\partial}{\partial y}(h(x,y)\cdot\bar{v})=0 \cdots\cdots\cdots\cdots(2)$$

In using Darcy's law, the details of the velocity profile through the thickness are neglected and the average velocities are used.

$$\bar{u} = -\frac{K_x}{\mu}\frac{\partial P}{\partial x}, \bar{v} = -\frac{K_y}{\mu}\frac{\partial P}{\partial y} \quad \cdots\cdots(3)$$

Substituting equation (3) into equation (2), the governing equation for the pressure distribution is given by ;

$$\frac{\partial}{\partial x}\left(h(x,y)\cdot\frac{K_x}{\mu}\frac{\partial P}{\partial x}\right)+\frac{\partial}{\partial y}\left(h(x,y)\cdot\frac{K_y}{\mu}\frac{\partial P}{\partial y}\right)=0 \quad \cdots\cdots(4)$$

$$\frac{\partial^2 P}{\partial x^2}+\frac{K_y}{K_x}\frac{\partial^2 P}{\partial x^2}+\frac{1}{h(x,y)}\frac{h(x,y)}{\partial x}\frac{\partial P}{\partial x} + \frac{K_y}{K_x}\frac{1}{h(x,y)}\frac{\partial h(x,y)}{\partial y}\frac{\partial P}{\partial y}=0 \quad \cdots\cdots(5)$$

The solution to equation (5) provides the pressure fields in the flow domain at given time. The boundary conditions are given by ;

(a) at the flow front; $P=0$ ·····(6a)

(b) at mold inlet ;

for constant pressure filling, $P=P_0$ .....(6b)

for constant flow rate filling,

$$-\frac{K}{\mu}\frac{\partial P}{\partial \bar{n}} = q \quad \cdots\cdots(6c)$$

(c) at mold boundaries ; $\frac{\partial P}{\partial \bar{n}} = 0$ ·····(6d)

A condition imposed at the moving front requires that the boundary propagates with the local fluid velocity at that surface. The local velocities are calculated from the superficial velocities of the fluid flows by using the following equations ;

$$v_f = \frac{dx_f}{dt} = \frac{v}{\varepsilon} \quad \cdots\cdots(7)$$

The porosity, ε, is required to convert the superficial velocity to a local velocity and determined from the properties of the fiber preform using the following equation ;

$$\varepsilon = 1 - \frac{\rho_b}{\rho_f} = 1 - \frac{N\xi_f}{h(x,y)\rho_f} \quad \cdots\cdots(8)$$

where ρ_b is the bulk density of the fiber preform inside the mold cavity and ρ_f is the density of fiber. N is the number of fiber mat, ξ_f is surface density of fiber mat and h(x,y) is the mold thickness. In case that the porosity and the mold thickness are invariant inside the mold, an expression for porosity is represented by more simpler form.

3. NUMERICAL METHODS

The main characteristics of the resin flow in a general two-dimensional mold are the advancement of the resin front and its arbitrary shaped boundaries. With traditional numerical approaches, special procedures are required at the boundaries and to deal with the moving front.

Although the mold filling process is not a steady state process, the mold filling can be regarded as a quasi-steady state process by assuming a steady state condition at each time step. The new flow front can be estimated according to the velocity vector of the flow front and the time step. This procedure of solving a steady state problem and flow front propagation is repeated until the mold is filled. Fig. 1 shows algorithm for simulating RTM mold filling using finite element methods and numerical mesh generation scheme presented here.

The modeling of the mold filling involves the collision of the fluid front with the solid walls. To deal with this extra difficulty, we have implemented an adaptive algorithm which relocates the nodes using mass conservation. Using this algorithm, we could find the contact point located at the intersection of the solid wall by minimizing the mass loss.

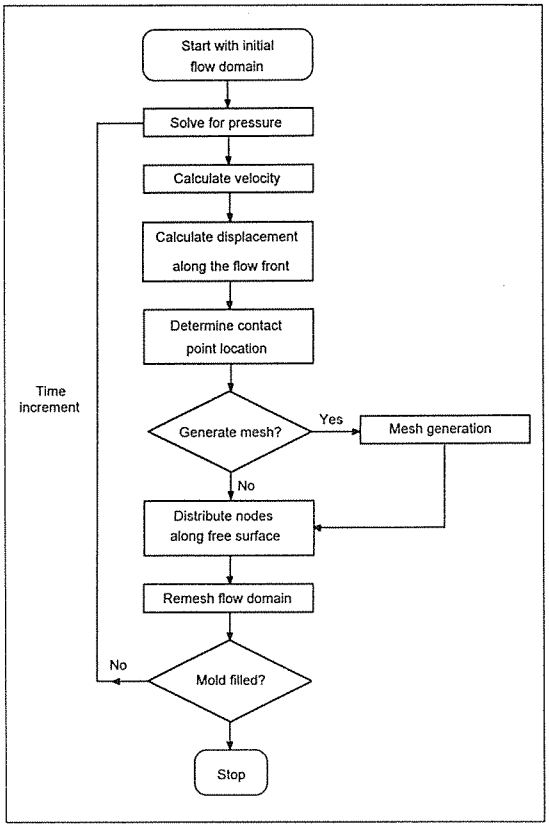

Fig. 1. Flow chart for numerical simulation of mold filling

Numerical mesh generation on any irregularly shaped geometry is performed by essentially mapping the boundaries of the physical domain to a more regular shape in computational domain. A mesh is created on the transformed, simpler domain and this can then be mapped back to provide a curvilinear mesh on the original irregular shape. The governing equations for mesh generation are similarly transformed and solved on the computational domain, using the well-established finite difference techniques, and the solutions at every node are mapped back onto the physical domain. Though several expressions are possible, Poisson type elliptic expressions are most commonly used to relate the physical (x, y) coordinates to the computational (ξ, η) coordinates due to their inherent smoothness and ability to handle boundary discontinuities. These relations are given as ;

$$\frac{\partial^2 \xi}{\partial x^2} + \frac{\partial^2 \xi}{\partial y^2} = P(\xi, \eta) \quad \cdots\cdots(9a)$$

$$\frac{\partial^2 \eta}{\partial x^2} + \frac{\partial^2 \eta}{\partial y^2} = Q(\xi, \eta) \quad \cdots\cdots(9b)$$

In the above equation P and Q are the grid control functions that can be used to specify mech concentration in desired areas. During the filling process, the flow domain continuously expands. A constant mesh size to cover this domain at all stages of filling could result in either too coarse meshes over large domains or in too fine meshes over small domains. Allowing the mesh size to be continuously expanded until the fluid fills the mold, the mesh is produced in a computationally economic way. This is implemented by adding a new curvilinear computational coordinate line to the flow domain each time the free surface passes a mold boundary node.

The governing equation has position dependent variables and the resin flow front is assumed to evolve during mold filling. These two characteristics can be conveniently handled by finite element formulation. Four-noded quadrilateral finite elements are used in this study. The pressure P and the velocity component u, v at a point in the finite element are

$$P=\sum_i^4 P_i \phi_i,\ u=\sum_i^4 u_i \phi_i,\ v=\sum_i^4 v_i \phi_i \quad \cdots\cdots(10)$$

By applying the Galerkin method to the governing equation, the following formulation is yielded.

$$<\phi_i : \frac{\partial^2 P}{\partial x^2} + \frac{K_y}{K_x}\frac{\partial^2 P}{\partial y^2} + \frac{1}{h(x,y)}\frac{\partial h(x,y)}{\partial x}\frac{\partial P}{\partial x}$$

$$+ \frac{K_y}{K_x}\frac{1}{h(x,y)}\frac{\partial h(x,y)}{\partial y}\frac{\partial P}{\partial y} >=0 \quad \cdots\cdots(11)$$

where the bracket denotes the integration over the domain. Performing the integration by parts on equation (11), and thereafter using the divergence theorem, one obtains the following matrix form equation, coefficient matrix and load vector.

$$[K] \cdot P = [F] \quad \cdots\cdots(12a)$$

$$[K] = k_{ij} = \int_{\Omega} \left[\frac{\partial \psi_i}{\partial x} \frac{\partial \psi_j}{\partial x} + \frac{K_y}{K_y} \frac{\partial \psi_i}{\partial y} \frac{\partial \psi_i}{\partial y} + \frac{1}{h(x,y)} \frac{\partial h(x,y)}{\partial x} \frac{\partial \psi_i}{\partial x} \cdot \psi_j + \frac{K_y}{K_y} \frac{1}{h(x,y)} \frac{\partial h(x,y)}{\partial y} \frac{\partial \psi_i}{\partial y} \cdot \psi_j \right] d\Omega \quad \cdots\cdots(12b)$$

$$[F] = f_i = \int_{\Gamma} \frac{\partial P}{\partial n} \cdot \psi_j d\Gamma \quad \cdots\cdots(12c)$$

Solution of the global matrix equation yields the pressure distribution in the flow domain at each time step. The velocity of each node is also obtained from the computed pressure of each node by use of equation (3).

4. RESULTS AND DISCUSSION

In order to predict the progression of flow front and to estimate what processing factors had influence on mold filling in RTM process, the numerical simulations based on the finite element method were performed. The material properties and processing conditions used for the simulation of mold filling were listed in Table 1.

4.1. Flow advancement by mesh generation in the mold with insert

The handling of multiply-connected domain such as the mold with insert was successful by using the computational program developed in the present study. It could be implemented for molds with dividing front lines or the case of weldlines where two separate portions of the resin front

Table 1. Materials properties and processing conditions used in the numerical simulations of mold filling

Materials Properties	fluid	unsaturated polyester
	viscosity	1 Pa · s
	fiber mat	glass, random
	permeability	$1.0 \times 10^{-9} m^2$
Processing Conditions	mold thickness	4mm
	inlet gate width	2cm
	fiber volume fraction	0.4
	inlet pressure	1.5×10^4Pa

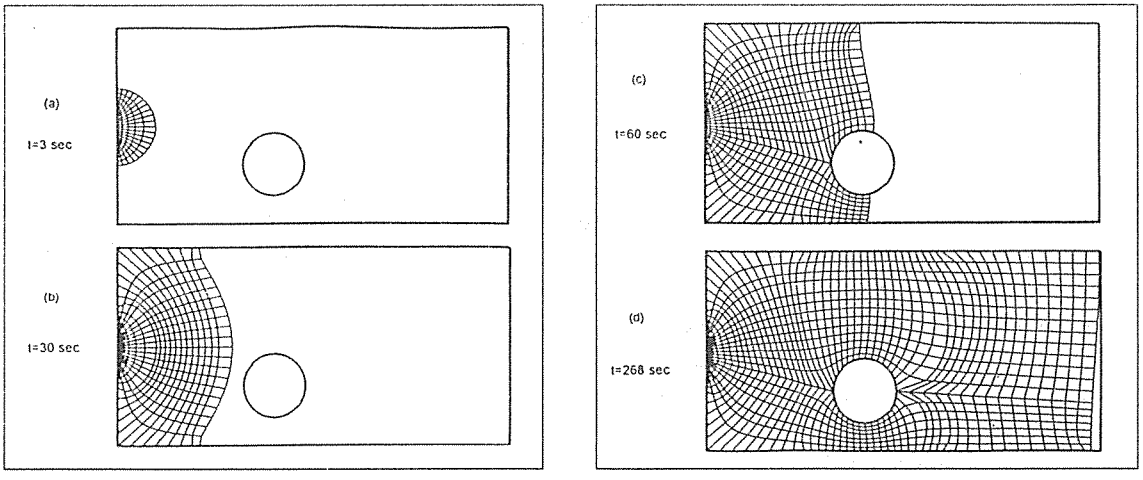

Fig. 2. Meshes generated during the filling of the mold with a circular insert (a) at t=3s, (b) at t=30s, (c) at t=60s, and (d) at t=268s

merged together. In finite element formulation, the merging of the flow fronts was automatically accounted for and posed no particular mathematical problem. But the mesh generatioon procedure for the mold containing interior obstacle was shown in Fig. 2(a)−(d) with the advancement of the flow front. The size of the mold was 30× 15(cm) and the radius of insert was 2.4 cm. At the biginning of injection, the number of element was 100(t=3s by extrapolation). This mesh was continuously enlarged to mesh size of 340 at t=30s. At the instant that the free surface contacted with inserted object, the mesh was generated by two steps, dividing the flow domains into two sections and this procedure was continued until the mold was filled. The predicted time for completely filling the mold was 274s.

4.2. Flow pattern varying with inlet conditions

The flow pattern under two cases of inlet condition were compared. As shown in Fig. 3(a), it was noted that the initial flow profiles of the resin front were a series of circles expected for isotropic preform under constant inlet pressure condition, and then the advancing flow front progressively straightened out during filling and later flattened against mold width. The temporal locations of the advancing flow fronts under the constant inlet flow rate of $3.0\times10^{7}m^{3}/s$ were

depicted in Fig. 3(b). Flow front distribution seemed to be more uniform than Fig. 3(a). The fluid volume between two front lines was expected to be the same. The numerically predicted fill time at which resin filled 99% of the mold volume was 347s and an extrapolated predicted fill time of t_{fill}= 350s was obtained. The exact fill time calculated using constant inlet flow rate and the available volume was 360s. A resulting error based on above analysis indicated approximately 2.8% for the present case. The error seemed to be within acceptable limits. The numerical mesh generation techniques used here resulted in typically less volumetric error because the fluid domain was meshed fully without interpolation.

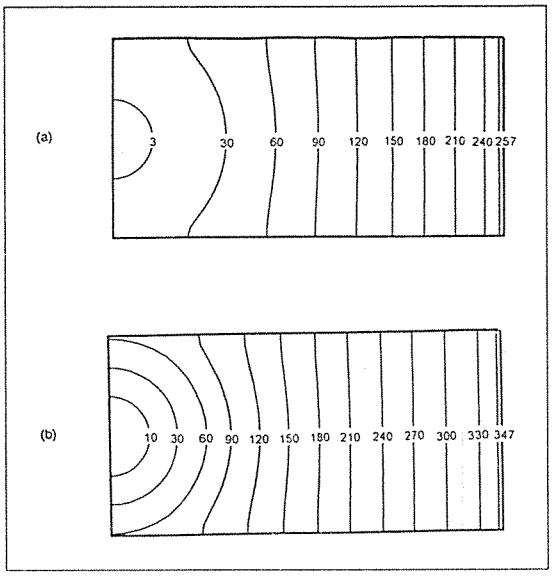

Fig. 3. The temporal locations of the advancing flow fronts (a) under constant pressure inlet condition (t_{fill}=261s), and (b) under constant flow rate inlet condition(t_{fill}= 350s)

4.3. Flow through the anisotropic preform

In order to investigate the filling of a square mold containing an anisotropic preform and to compare with the isotropic case, the next set of results was presented. Other processing conditions used for this case were the same as discussed above. Fig. 4(a) showed the results of isotropic preform and the fill time was predicted as 419s. We defined the degree of anisotropy as K_x/K_y. In case of the degree of anisotropy equal to 2, the predicted fill time was 505s as shown in Fig 4(b). The flow progression clearly showed the relative ease of resin movement in x−direction as compared with that in y−direction. The decrease in K_y resulted in a more elongated flow pattern along the flow direction and led to much slower movement of the resin front. Therefore, the mold fill time under identical x-directional permeability was longer with the increase of the degree of

anisotropy, and further the anisotropic nature of the fabric caused a large change in the shape of the evolving flow front.

4.4. The effect of different permeability

In order to investigate the effects of installment of fiber mats with different permeability within a mold, numerical simulations were performed for two contradictory configurations. The results for molds with two regions having different permeability were presented in Figs. 5 and 6. The permeability variation could be created by adding fiber mats of different structure, but local fiber volume fraction was assumed constant. Fig. 5 was the case that the fabric mat having the higher permeability was located at near inlet gate. Fig. 6 was vice versa. The predicted fill time for the former case was 247s and the latter was 232s. At first glance, the installment of fiber mats of the latter case was more favorable as far as fill time was concerned. This behavior was explained as the reduction of pressure gradient with progression of the flow front. The reduction of pressure gradient in the distant region from inlet gate caused to lessen driving force for flow to advance.

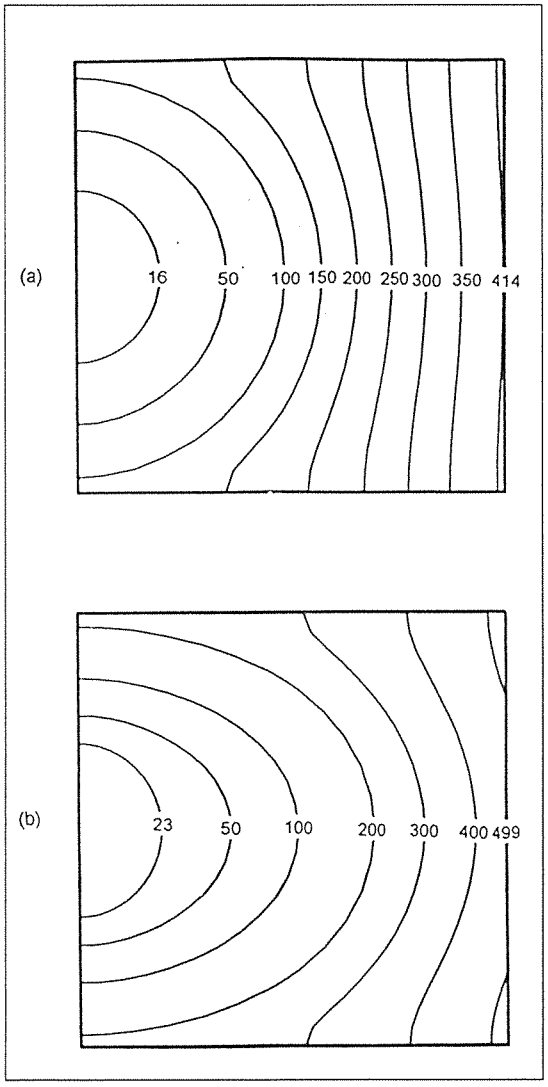

Fig. 4. Effects of degree of anisotropy for squared mold (where $K_x=1.0\times10^{9}m^2$) ; (a) $K_x/K_y=1$ ($t_{fill}=419s$), (b)$K_x/K_y=2$($t_{fill}=505s$)

4.5. The effect of gate location

To investigate the effect of gate location, we

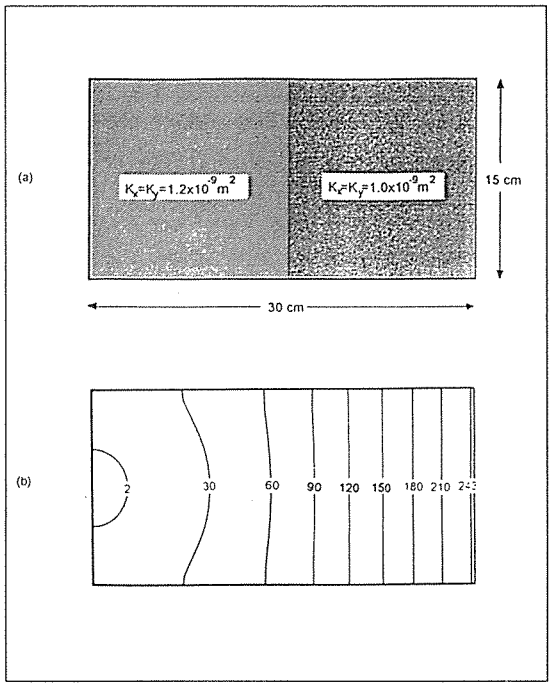

Fig. 5. Mold configuration with regions of different permeabilities ;
(a) fiber mat arrangement with high and low permeability in sequence,
(b) flow front locations ($t_{fill}=247s$)

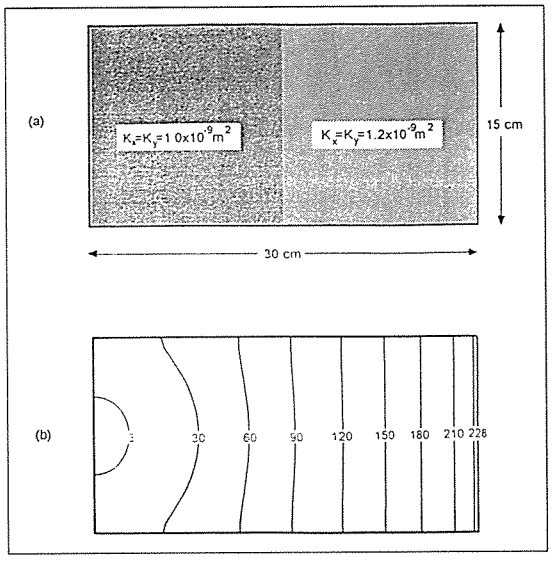

Fig. 6. Mold configuration with regions of different permeabilities ;
(a) fiber mat arrangement with low and high permeability in sequence,
(b) flow front locations (t_{fill}=232s)

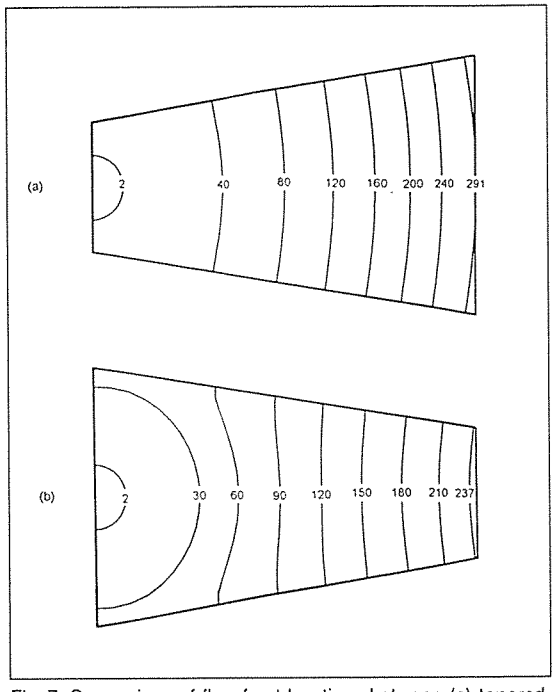

Fig. 7. Comparison of flow front locations between (a) tapered-diverged (t_{fill}=300s) and (b) tapered-converged mold (t_{fill}=241s)

prepared two cases of mold as shown in Fig. 7(a) and 7(b), either to fill the section from the larger side to the smaller side, or vice versa. The results of filling time were obtained t_{fill}=300s and in latter case t_{fill}=241s. From these results, the arrangement of flow front from the large side to the small side was advantageous since less fill time was required. The driving force for flow was the pressure gradient and the pressure gradient was reduced with the flow progression. Since the free surface was forced to advance flow front, it was important to keep the line of the free surface shorter at region distant from inlet gate. Therefore, it was concluded that it was much easier to fill a mold if the line of free surface was reduced gradually.

4.6. Mold flow with variable thickness and fiber volume fraction

We studied in case that the thickness of the mold was gradually increased or decreased along the flow direction. Results of numerical simulation were presented for two conditions ; one with a constant fiber volume fraction, the other with a variable fiber volume fraction. Constant fiber volume fraction was accomplished by altering the number of fiber mats. Variable fiber volume fraction was obtained by fixing the number of fiber mats in a mold. In industrial practice, these variations could be either intentional or due to difficulties of processing.

Under the condition of constant fiber volume, the predicted fill time of the mold with increasing thickness was 232s, while for the mold with decreasing thickness it was 289s. Comparing between two molds, the mold with increasing thickness had advantage in saving the fill time. It was clear that initially when the flow began, there was no significant difference between these two cases but the large difference in filling configuration happened in the case of long flow distance. From Hele-shaw flow equations, it was clear that

the velocities were in proportion to mold thickness. In addition, the flow process treated with constant pressure condition revealed that at the beginning of filling, the pressure gradient reached highest and as the mold was filled, the pressure gradient decreased slowly and seemed to be constant. This led to gradual reduction of the flow rate. Since the pressure gradient dropped in long flow distance and the fluidity also went down notably in the region of reduced thickness, the mold with decreasing thickness required much more fill time.

Under variable fiber volume fraction condition, the fiber volume fraction was 50% in the reduced thickness region and 30% in the expanded thickness region. Therefore, the averaged fiber volume fraction throughout the mold maintained 40% as the same condition of constant fiber volume fraction.

To account for varying fiber volume fraction, the permeability equation as a function of fiber volume fraction was introduced. Here, it was assumed that Carman-Kozeny equation could satisfy the relationship between permeability and fiber volume fraction in this range of fiber volume fraction[15-17]. This Carman-Kozeny equation is expressed as ;

$$K = \frac{r_f^2}{k'} \frac{(1-V_f)^3}{V_f^2} \quad \cdots\cdots(15)$$

where k' is the Kozeny constant which accounts for tortuosity and pore non uniformity. Although the permeability might not match Carman-Kozeny relationship well as a function of the fiber volume fraction, this could account for the change of permeability in the varying thickness section. Kozeny constant value was selected 0.01 in order to match permeability to $1.0\times10^{9}m^2$ at V_f=0.4 as the representative value. Since the preform was assumed as continuous and random glass fiber mat, the value of the radius of fiber in Carman-Kozeny equation was determined as 5.65

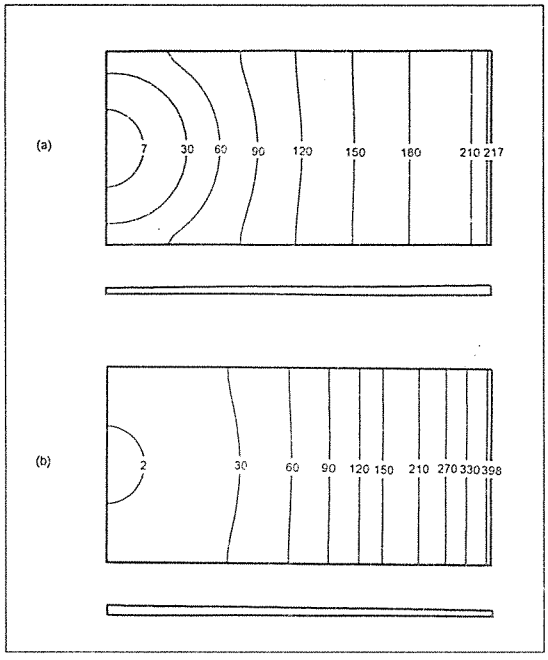

Fig. 8. Variable thickness mold with variable fiber volume fraction ;
(a) increasing thickness (t_{fill}=219s), (b) decreasing thickness (t_{fill}=413s).

$\times10^{6}m$. Fig. 8 showed the results for this simulation. For the mold with increasing thickness the predicted fill time was 219s, while for the mold with decreasing thickness it was 413s. Fig. 8 showed that there was more decrease in flow velocity in the reduced thickness area and the flow front progresses faster than in the expanded thickness area. The flow slowed down significantly when it reached the reduced thickness area. There was more resistance to flow as the permeability was considerably low in this area due to high fiber volume fraction. It could be concluded that these differences of mold configuration had great influences on the flow field and processing cycle.

5. CONCLUSIONS

Computational program was developed for the

numerical simulation of mold filling in the RTM process. The Galerkin finite element method and the numerical mesh generation can handle the changing flow domain shape during mold filling. This program can be also applied to the irregularly-shaped molds and molds with varying thickness under variable processing conditions.

Several key processing variables have been analyzed which influence on the behavior of mold filling in the RTM process. Numerical simulations helped identify the variables that controlled the resin flow and provided the guidelines of mold design. Several design principles were suggested by application examples. The resin flow should be arranged (a)from low permeability region to high permeability region, (b)from larger side to smaller side in the tapered mold, (c)from thin thickness to thick thickness in the variable thickness mold, and (d)the insert should be located in far away the inlet gate.

NOMENCLATURE

h(x,y)	mold thickness
J	transformation Jacobian
K_x, K_y	permeabilities in x,y directions
k′	Kozeny constant
N	number of fiber mats
P	pressure
$P(\xi,\eta)$	grid control function
$Q(\xi,\eta)$	grid control function
u, v, w	x−, y−, z−directional velocity components
V_f	volume fraction of fiber
x, y, z	global coordinates

Greek letters

ε	porosity
η	transformed coordinate
μ	viscosity
ξ	tranfromed coordinate
ξ_f	surface density of fiber mat
ρ_b	bulk density of fiber
ρ_f	density of fiber

REFERENCES

1. Owen, M.J., Rudd, C.D. and Middleton, V., "Effects of Process Variables on Cycle Time During Resin Transfer Molding for High Volume Manufacture," Materials Science and Technology, Vol.6, 1990, p. 656.

2. Karbhari, V.M., Slotte, S.G., Steenkamer, D.A. and Wilkins, D.J., "Effects of Materials, Process, and Equipment Variables on the Performance of Resin Transfer Molded Parts," Composites Manufacturing, Vol.3, No.3, 1992, p. 143.

3. Hayward, J.S. and Harris, B., "Processing Factors Affecting the Quality of Resin Transfer Moulded Composites," Plastics and Rubber Processing and Applications, Vol.11, No.4, 1989, p. 191.

4. Hayward, J.S. and Harris, B., "Effect of Process Variables on the Quality of RTM Mouldings," SAMPE Journal, Vol.26, No.3, 1990, p. 39.

5. Stover, D., "Resin Transfer Molding for Advanced Composites," Advanced Composites, March/April, 1990, p. 60.

6. Coulter, J.P., Smith, B.F. and Guceri, S.I., "Experimental and Numerical Analysis of Resin Impregnation During the Manufacturing of Composite Materials," Proc. 2nd Tech. Conf., ASC, 1987, p. 209.

7. Coulter, J.P. and Guceri, S.I., "Resin Impregnation During the Manufacturing of Composite Materials Suject to Prescribed Injection Rate," J. of Reinforced Plastics and Composites, Vol.7, 1988, p. 200.

8. Coulter, J.P. and Guceri, S.I., "Resin Impregnation During Composites Manufacturing: Theory and Experimentation," Composites Sci. and Tech., Vol.35, 1989, p. 317.

9. Gauvin, R. and Chibani, M., "Modeling of Mold Filling in Resin Transfer Molding," Int.

Polym. Processing, Vol.1, No.1, 1986, p. 42.
10. Li, S. and Gauvin, R., "Numerical Analysis of the Resin Flow in Resin Transfer Molding," J. of Reinforced Plastics and Composites, Vol.10, 1991, p. 314.
11. Trochu, F. and Gauvin, R., "Limitations of a Boundary-Fitted Finite Difference Method for the Simulation of the Resin Transfer Molding Process," J. of Reinforced Plastics and Composites, Vol.11, 1992, p. 772.
12. Bruschuke, M.V. and Advani, S.G., "A Finite Element/Control Volume Approach to Mold Filling in Anisotropic Porous Media," Polymer Composites, Vol.11, No.6, 1990, p. 398.
13. Bruschuke, M.V. and Advani, S.G., "RTM: Filling Simulation of Complex Three Dimensional Shell-like Structure," SAMPE Quarterly, October, 1991, p. 2.
14. Cai, Z., "Analysis of Mold Filling in RTM Process," J. of Composite Materials, Vol.26, No.9, 1992, p. 1310.
15. Skartisis, L., Kardos, J.L. and Khomami, B., "Resin Flow Through Fiber Beds During Composite Manufacturing Processes. Part I: Review of Newtonian Flow Through Fiber Beds," Polym. Eng. Sci., Vol.32, No.4, 1992, p. 1.
16. Adams, K.L. and Rebenfeld, L., "In-Plane of Fluids in Fabrics: Structure/Flow Characterization," Textile Research Journal, Vol.57, 1987, p. 647.
17. Williams, J.G., Morris, C.E.M. and Ennis, B.C., "Liquid Flow Through Aligned Fiber Beds," Polym. Eng. Sci., Vol.14, No.6, 1974, p. 413.